Modeling flow in naturally fractured reservoirs
effect of fracture aperture distribution on dominant sub-network for flow

Gong, J.; Rossen, W. R.

DOI
10.1007/s12182-016-0132-3

Publication date
2017

Document Version
Final published version

Published in
Petroleum Science

Pet. Sci. (2017) 14:138–154
DOI 10.1007/s12182-016-0132-3

ORIGINAL PAPER

Modeling flow in naturally fractured reservoirs: effect of fracture aperture distribution on dominant sub-network for flow

J. Gong[1] · W. R. Rossen[1]

Received: 12 January 2016 / Published online: 17 December 2016

Abstract Fracture network connectivity and aperture (or conductivity) distribution are two crucial features controlling flow behavior of naturally fractured reservoirs. The effect of connectivity on flow properties is well documented. In this paper, however, we focus here on the influence of fracture aperture distribution. We model a two-dimensional fractured reservoir in which the matrix is impermeable and the fractures are well connected. The fractures obey a power-law length distribution, as observed in natural fracture networks. For the aperture distribution, since the information from subsurface fracture networks is limited, we test a number of cases: log-normal distributions (from narrow to broad), power-law distributions (from narrow to broad), and one case where the aperture is proportional to the fracture length. We find that even a well-connected fracture network can behave like a much sparser network when the aperture distribution is broad enough ($\alpha \leq 2$ for power-law aperture distributions and $\sigma \geq 0.4$ for log-normal aperture distributions). Specifically, most fractures can be eliminated leaving the remaining dominant sub-network with 90% of the permeability of the original fracture network. We determine how broad the aperture distribution must be to approach this behavior and the dependence of the dominant sub-network on the parameters of the aperture distribution. We also explore whether one can identify the dominant sub-network without doing flow calculations.

✉ J. Gong
J.Gong@tudelft.nl

[1] Department of Geoscience and Engineering, Delft University of Technology, 2628 CN Delft, The Netherlands

Edited by Yan-Hua Sun

Keywords Naturally fractured reservoir · Non-uniform flow · Effective permeability · Percolation · Waterflood

1 Introduction

A large number of oil and gas reservoirs across the world are naturally fractured and produce significant oil and gas (Saidi 1987). Efficient exploitation of these reservoirs requires accurate reservoir simulation. Naturally fractured reservoirs, like all reservoirs, are exploited in two stages: primary recovery and secondary recovery [sometimes followed by tertiary recovery, i.e., enhanced oil recovery (EOR)], with different recovery mechanisms. During primary production, the reservoir is produced by fluid expansion. In secondary production and EOR, since the fractures are much more permeable than the matrix, the injected water or EOR agent flows rapidly through the fracture network and surrounds the matrix blocks. Oil recovery then depends on efficient delivery of water or EOR agent to the matrix through the fracture network. Dual-porosity/dual-permeability models are still the most widely used methods for field-scale fractured-reservoir simulation, as they address the dual-porosity nature of fractured reservoirs and are computationally cheaper, although they are much simplified characterizations of naturally fractured reservoirs. To generate a dual-porosity/dual-permeability model, it is necessary to define average properties for each grid cell, such as porosity, permeability, matrix-fracture interaction parameters (typical fracture spacing, matrix-block size or shape factor), etc. (Dershowitz et al. 2000). Therefore, the fracture network used to generate the dual-porosity model parameters is crucial. Homogenization and other modeling approaches likewise require one to designate a typical fracture spacing

(Salimi 2010). The hierarchical fracture model (Lee et al. 2001) also requires that one define effective properties of the matrix blocks and fractures which are too small to be represented explicitly.

This paper is the first part of a three-part study showing that the appropriate characterization of a fractured reservoir differs with the recovery process. In this paper, we show that even in a well-connected fracture network, far above the percolation threshold, flow may be so unequally distributed that most of the network can be excluded without significantly reducing the effective permeability of the fracture network. The implications of this finding for characterization of naturally fractured reservoirs are the subject of parts two and three. Briefly, in primary production, any fracture much more permeable than the matrix provides a path for escape of fluids, while in waterflood or EOR, the fractures that carry most injected water or EOR agent play a dominant role. In this paper, we restrict our attention to flow of injected fluids, as a first step toward modeling recovery processes that depend on contact of injected fluids with matrix.

Field studies and laboratory experiments show flow channeling in individual fractures and highly preferential flow paths in fracture networks (Neretnieks et al. 1982; Neretnieks 1993; Tsang and Neretnieks 1998). Cacas et al. (1990a, b) proposed that a broad distribution of fracture conductivities is the main cause of the high degree of flow channeling. In order to understand these phenomena, many theoretical studies have been done. The separate influences of fracture network connectivity distributions (Robinson 1983, 1984; Hestir and Long 1990; Balberg et al. 1991; Berkowitz and Balberg 1993; Berkowitz 1995; Berkowitz and Scher 1997, 1998; de Dreuzy et al. 2001a) and fracture conductivity distributions (Charlaix et al. 1987; Nordqvist et al. 1996; Tsang et al. 1988; Tsang and Tsang 1987) on flow channeling have been considered and also the interplay of these two key factors (Margolin et al. 1998; de Dreuzy et al. 2001b, 2002). Berkowitz (2002) further pointed out that even a well-connected fracture network can exhibit sparse preferential flow paths if the distribution of fracture conductivities is sufficiently broad. Katz and Thompson (1987) proposed a similar finding for pore networks. Although the "unimportant" fractures carry little flow, they still can be important to the connectivity and the preferential flow paths. It is not clear whether one can eliminate those "unimportant" fractures without significantly affecting the flow properties of the fracture network. Also, how broad must the distribution of fracture conductivities be to obtain this result is still an open question.

We propose that, for the dual-porosity/dual-permeability simulation of a waterflooding process or EOR or in homogenization, for the purpose of modeling the fluid exchange between fractures and matrix blocks, only the sub-network which carries by far most of the injected water is of primary importance in characterizing the reservoir. It is important to understand the factors that influence the sub-network. Since the effect of fracture connectivity on flow properties of fracture networks is well discussed, we focus here on the influence of fracture aperture (i.e., fracture conductivity) distribution.

As the first step in our research, in this work we systematically study the influence of the fracture aperture distribution on the dominant sub-network for flow. In this work, we define "the dominant sub-network" as the sub-network obtained by eliminating a portion of fractures while retaining 90% of the original network equivalent permeability. In other words, we are interested in how broad the aperture distribution must be that a well-connected fracture network can exhibit a sparse dominant sub-network with nearly the same permeability. The properties of the dominant sub-network are also examined. If the fracture network is poorly connected, i.e., near the percolation threshold, it is well established that only a small portion of the fractures connects the injection well and the production well. Here we focus on well-connected fracture networks. Since information on fracture apertures, especially in the subsurface, is limited, we test power-law distributions (from narrow to broad), log-normal distributions (from narrow to broad), and one case in which the aperture is proportional to the fracture length.

This report is organized as follows: In Sect. 2, we introduce the numerical model and the research process of this study. In Sect. 3, we analyze the dominant sub-network. In Sect. 4, the possibility of identifying the dominant sub-network without doing flow simulations is discussed. Our conclusions are summarized in the last section.

2 Numerical model and research process

2.1 Numerical model

For simplicity in this initial study, we examine flow in a quasi-two-dimensional fractured reservoir. We use the commercial fractured-reservoir simulator FracMan^{TM} (Dershowitz et al. 2011) to generate fracture networks. A 3D fracture network is generated in a 10 m $\times$ 10 m $\times$ 0.01 m region. The shape of each fracture is a rectangle. Each fracture is perpendicular to the plane along the flow direction and penetrates the top and bottom boundaries of the region. The enhanced Baecher model is employed to allocate the location of fractures. Two fracture sets which are nearly orthogonal to each other are assumed, with almost equal numbers of fractures in the two sets.

Because of the uncertainties in data and the influence of cutoffs in measurements, in previous studies fracture-trace

lengths have been described by exponential, log-normal, and power-law distributions (Segall and Pollard 1983; Rouleau and Gale 1985; Bour and Davy 1997). Currently, a power-law distribution is assumed by many researchers to be the correct model for fracture length (Nicol et al. 1996; Odling 1997; de Dreuzy et al. 2001a, b), with exponent α ranging from 1.5 to 3.5. As proposed by de Dreuzy, if α is less than 2, flow is mostly channeled into longer fractures. On the other hand, if α is larger than 3, fracture networks are essentially made up of short fractures. For α in a range of 2–3, both long and short fractures contribute to the flow. We set $\alpha = 2$ which is a reasonable value in the real world. For this value of α, both short and long fractures make contribution to the flow through the fracture network. In this study, the fracture length follows a power-law distribution ($p(x)$):

$$p(x) = \frac{\alpha - 1}{x_{\min}} \left(\frac{x_{\min}}{x}\right)^{\alpha} \quad (1)$$

where $p(x)$ is the probability density function for a fracture of length x; α is the power-law exponent (i.e., 2); x is the fracture length; and $x_{\min}$ the lower bound on x, which we take to be 0.2 m. We truncate the length distribution on the upper end at 6 m; thus, there are no extremely short or long fractures. In particular, the opposite sides of our region of interest cannot be connected by a single fracture. Since even the smallest fracture is much taller than the thickness of the region of interest (0.01 m), and there is no change of the model in the Z direction, the 3D model is in essence of a 2D fracture network.

For fracture apertures, we adopt two kinds of distributions which have been proposed in previous studies: power-law and log-normal. In each kind of distribution, a range of parameter values are examined. The aperture is randomly assigned to each fracture. In the case where the aperture is proportional to the fracture length, the fracture aperture follows the same power-law distribution as fracture length. The details of the aperture distribution are introduced below.

To focus on the influence of fracture aperture distributions on the dominant sub-network, except for the aperture distribution, all the other parameters remain the same for all the cases tested in this study, including fracture length, orientation, etc.

2.2 Flow simulation model

We assume that a fracture can be approximated as the slit between a pair of smooth, parallel plates; thus, the aperture of each fracture is uniform. The dependence of fracture permeability (k) on aperture (d) is defined as: $k = d^2/12$, where k is defined based on the cross-sectional area of the fracture. Steady-state flow through a 10 m × 10 m × 0.01 m fractured rock mass is considered. In this paper, we assume that the fracture permeability is much greater than the matrix permeability, which is common in fractured reservoirs (van Golf-Racht 1982; Nick et al. 2011). The flow regimes of highly fractured rock mass can be characterized by the fracture-matrix permeability ratio. If the ratio is greater than 10^5–10^6, fractures carry nearly all the flow (Matthai and Belayneh 2004; Matthai and Nick 2009). Since we are interested in the non-uniform flow in well-connected fracture networks, for simplicity we assume that the matrix is impermeable; fluid flow takes place only in the fracture network. For computing flow in discrete fracture networks, as in most numerical simulation methods, Darcy's law for steady-state incompressible flow is employed, and mass is conserved at each intersection of fractures. In our models, we induce fluid flow from the left side to the right side by applying a constant difference in hydraulic head across the domain while all the other boundaries are impermeable. The equivalent permeability of the fracture network K (in m^2) is defined by.

$$K = \frac{Q/(LW)}{\Delta h/L} \cdot \frac{\mu}{\rho g} \quad (2)$$

where Q is the volumetric flow rate, m^3/s; L is the length of the square region, m; W is the thickness of the region, m; μ is the fluid viscosity, Pa s; ρ is the fluid density, kg/m^3; g is the acceleration due to gravity, m/s^2; Δh is the difference in hydraulic head between inflow and outflow boundaries; and in petroleum engineering, this is equal to $\Delta p/\rho g$, where Δp is the pressure difference, Pa.

Mafic™, a companion program of FracMan™, is employed to simulate flow in the fracture networks.

2.3 Methodology

As mentioned above, we believe that when the aperture distribution is broad enough, there is a dominant sub-network which approximates the permeability of the entire fracture network. Our main interest lies in examining the influence of the aperture distribution (the exponent α in a power-law distribution and the standard deviation σ in a log-normal distribution) on the dominant sub-network. Countless criteria can be used to decide which portion of fractures to remove, such as fracture length, aperture, [length × aperture], velocity, etc. Here we choose a criterion based on the flow simulation results. Mafic™ subdivides the fractures into finite elements for the flow calculations. The flow velocity at the center of each finite element and the product of flow velocity and aperture (Q_{nodal}) can be obtained. Based on this value, we compute the average value (Q) of all the elements in each fracture. Q is then used as the criterion to eliminate fractures: Fractures are eliminated in order, starting from the one

with the smallest value of Q to the one with the largest value of Q. After each step, we calculate the equivalent network permeability of the truncated network. It should be noted that the elimination of fractures is based on the flow in the original fracture network, not the truncated network.

We also describe the properties of the "backbone," i.e., the set of fracture segments that conduct flow, specifically its aperture distribution. The backbone is determined by removing fractures which do not belong to the spanning cluster, as well as dead ends. In other words, the backbone is formed by the fracture segments with nonzero Q. The dead ends are often parts of a fracture rather than the entire fracture. In order to describe the properties of the conducting backbone, we reduce the fracture network to its backbone at the start and at each step after eliminating fractures.

Because the generation of the fracture network is a random process, an infinite number of fracture networks could be generated with the same parameter values for the density, orientation, fracture length, and the aperture distribution. In this study, for each set of parameter values, we generate one hundred realizations.

2.4 Percolation theory

Percolation theory is a powerful mathematical tool to analyze transport in complex systems (Aharony and Stauffer 2003; Sahimi 2011). It has been widely used to describe the connectivity and the conductivity of fracture networks.

Our research focuses on well-connected fracture networks, so we employ percolation theory here to analyze the connectivity of the initial fracture network, to illustrate how far above percolation threshold, and how well connected, the initial fracture network is.

The simplest percolation models are site percolation and bond percolation, in which sites or bonds on an infinite lattice are occupied and open to flow with a probability p. To analyze a fracture network, continuum percolation is more applicable, in which fractures can be placed anywhere and can be of variable length. To analyze the connectivity of a fracture network using percolation theory, one must choose a parameter equivalent to the occupancy probability used in site or bond percolation. Different choices have been considered in previous studies. The first choice is the average number of intersections per fracture (Robinson 1983). A second choice is the number of fractures in the system (Balberg et al. 1991; Berkowitz 1995). A third choice is the dimensionless density, defined as $p = Nl^2/L^2$, where N is the number of fractures, l is the (uniform) fracture length, and L is the system size (Bour and Davy 1997). A fourth choice is the probability that a point is within the effective area of a fracture (Masihi et al. 2005, 2008). As the fracture networks used in this study are generated using the enhanced Baecher model, in which the fracture centers are located using a Poisson process, we choose the fourth option described above as the percolation parameter p:

$$p = 1 - \exp\left(\frac{-N\langle a_{\mathrm{ex}}\rangle}{4L^2}\right) \tag{3}$$

where N is the number of fractures in the system and $\langle a_{\mathrm{ex}}\rangle$ is the average excluded area. Excluded area is defined as the area around a fracture in which the center of other fractures cannot lie in order to ensure the fractures do not intersect (Balberg et al. 1984). For fracture networks comprising two orthogonal fracture sets of uniform fracture length l, the average excluded area is defined as (Belayneh et al. 2006).

$$\langle a_{\mathrm{ex}}\rangle = l^2/2 \tag{4}$$

Masihi et al. (2008) proposed that if a fracture network has a distribution of fracture lengths, its connectivity is identical to that of a system with fixed fracture length equaling to the so-called effective length l_{eff}, which is the root-mean-square fracture length:

$$l_{\mathrm{eff}}^2 = \langle l^2\rangle \tag{5}$$

The percolation threshold p_c is the value at which a cluster of fractures connects the opposite sides of the region. The threshold value is affected by the position, orientation, and length distribution of fractures, the system size, etc. Masihi et al. (2008) studied the percolation threshold of fracture networks with different fracture-length distributions and different system sizes. For fracture networks generated in a 10 m $\times$ 10 m region with random orientation, when the length follows a power-law distribution with exponent $\alpha = 2$, they proposed that the percolation threshold is around 0.66. In our case, the system size and the power-law exponent are consistent with their work, but the fractures are not randomly orientated, but in two perpendicular sets. As suggested by Masihi et al. (2005, 2008), the percolation threshold for a fracture network with two perpendicular fracture sets is lower than that for a model with randomly oriented fractures. Also, the truncation of the fracture-length distribution impacts the threshold value. Since the percolation threshold value is not our focus, here we consider 0.5–0.7 as a reasonable estimate of the percolation threshold. For the cases we study here, the value of the percolation parameter p of initial fracture networks is around 0.9. Considering the definition of p in Eq. (4), a value $p = 1$ corresponds to infinite fracture density (zero probability of not intersecting another fracture). Thus, our fracture network is far above the percolation threshold and is well connected.

3 Identifying the dominant sub-network based on flow simulation results

3.1 Models without correlation between fracture aperture and length

3.1.1 Power-law aperture distribution

Some field observations and experimental studies show that a power-law distribution can describe the fracture-aperture distribution, although the available data are limited, especially from subsurface populations (Barton et al. 1989; Wong et al. 1989; Barton and Zoback 1992; Belfield and Sovich 1994; Marrett 1996). The power-law probability density function for aperture d is:

$$p(d) = d^{-\alpha} \tag{6}$$

If the power-law aperture distribution is described by Eq. (6), the studies cited above find that the value of the exponent α in nature is 1.0, 1.1, 1.8, 2.2, or 2.8. In this study, the power-law aperture distribution with a lower bound follows the form of Eq. (1), in which α should be larger than 1. To include the entire range of feasible cases (from narrow to broad aperture distribution), here we examine α in the range from 1.001 to 6. In each case, the fracture aperture is limited to the interval between 0.01 and 10 mm. Because of this truncation, as the exponent α increases from 1 to 6, the fracture apertures concentrate in a narrow range near the lower limit (Fig. 1). For $\alpha = 1.001$, the apertures occupy the entire range from 0.01 to 10 mm: The difference between the smallest and the largest aperture is nearly three orders of magnitude. For $\alpha = 4$ to 6, most apertures lie between 0.01 and 0.03 mm. The absolute magnitude of aperture is not important in the dimensionless results to follow, but a narrow range of apertures does affect the results.

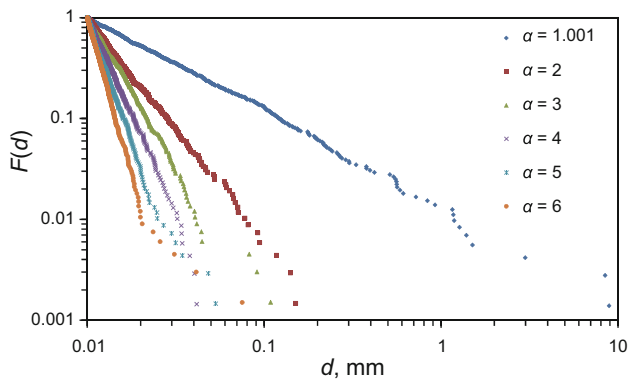

Fig. 1 Fraction of fractures F with aperture (d) larger than the given value, for power-law distributions with different values of the exponent α

In this paper, we mainly show the results for α with values 1.001, 2, and 6. The results for α with additional values examined in this study can be found elsewhere (Gong and Rossen 2015).

After running flow simulations on the percolation cluster of the original fracture network, we determine the value of Q for each fracture. The fractures with the smallest Q are eliminated first, then the larger ones. After a given number (10) of fractures are eliminated, we calculate the permeability of the remaining network and the cumulative length of the conducting backbone, l_b, in that network. We then eliminate ten more fractures and repeat until the network becomes disconnected. The normalized equivalent permeability of the truncated fracture network is shown in Fig. 2 for all 100 realizations for α with values 1.001, 2, and 6. The scatter in Fig. 2 reflects differences among the realizations. The red curve in each case shows the average trend through the 100 realizations. Figure 3 shows the comparison of this average trend for the different values of α ($\alpha = 1.001$ to 6). The results show that for all of the cases, a portion of fractures can be eliminated without significantly affecting the overall network permeability. Particularly, when the power-law aperture distribution exponent $\alpha = 1.001$, the cumulative length of the conducting backbone of the truncated fracture network which retains 90% of the original-network equivalent permeability is roughly 30% of the total fracture length of the original fracture network. That is, there is a sparse sub-network which carries almost all the flow and can be a good approximation of the original fracture network. We call this sub-network retaining 90% of the original equivalent permeability the dominant sub-network. As exponent α increases from 1.001 to 6, the dominant sub-network becomes denser, and the length of the pathway becomes longer. For $\alpha = 2$, about 50% of fracture length can be removed while retaining 90% of the original permeability. In the case of $\alpha = 6$, the cumulative length of the conducting backbone of the dominant sub-network is around 60% of the total length of the original fracture network. It is worth noting that the largest ratio of l_b/l_o for all the cases is around 0.8, reflecting the length of dangling and dead ends in the original fracture network, which represents about 20% of its total length.

If we compare cases with aperture distributions from narrow to broad, we find that when the aperture distribution is broad ($\alpha \leq 2$), most of the fractures can be eliminated without significantly affecting the equivalent permeability: The fracture network behaves as a sparser sub-network. As the aperture distribution becomes narrower (α increase from 1.001 to 6), to retain a certain percent of the original fracture network permeability, more fractures are needed (Fig. 3).

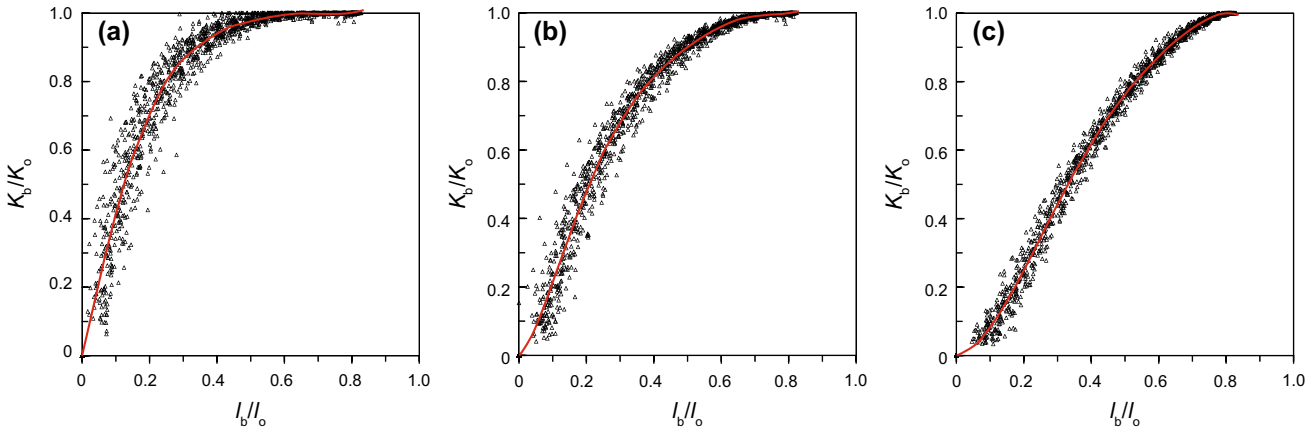

Fig. 2 Sub-network equivalent permeability (K_b) normalized by the equivalent permeability of the original fracture network (K_o), plotted against the length of the backbone of the truncated fracture network (l_b) normalized by the total length of the original fracture network (l_o): power-law aperture distributions with $\alpha = 1.001$ (**a**), $\alpha = 2$ (**b**), $\alpha = 6$ (**c**). Results of 100 realizations are shown for each value of α. The *red curve* is the average trend curve

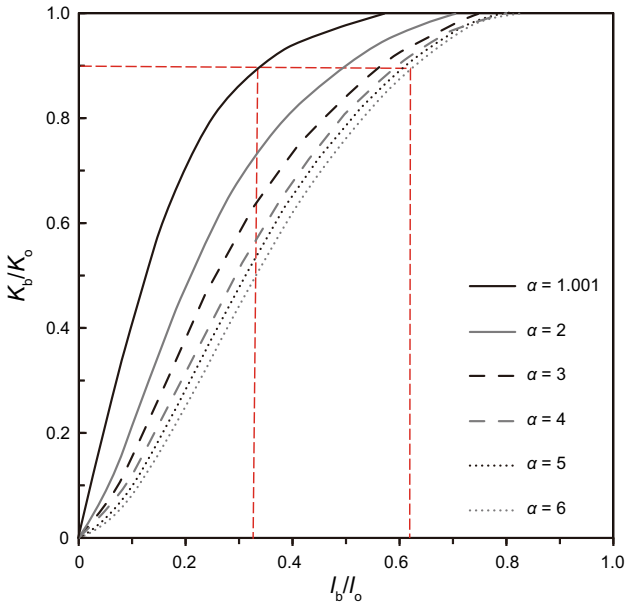

Fig. 3 Average curves from Fig. 2, including additional values of α

In the network, some subsets of fractures do not participate in fluid flow; these are known as dead-end or dangling fractures. To identify the flow structure in fracture networks, the backbone of the original fracture network and its sub-network is determined by removing fractures which do not belong to the spanning cluster, as well as dead ends (Fig. 4). As presented in Fig. 4, the structure of the sub-network that retains 90% of the original equivalent network permeability depends on α. For $\alpha = 1.001$ (Fig. 4b), the backbone is much sparser than that for larger values of α, because many more fractures can be removed without reducing the permeability greatly.

For this initial study, for simplicity, we chose to study a 10 m × 10 m region with no-flow boundaries on top and bottom in Fig. 4. As a result, the region near those boundaries shows fewer fractures in the dominant sub-network. However, Fig. 4 suggests that the size of the region affected by the boundaries is limited, and that the main conclusion of our work is that most flow passes through relatively few fractures, and the remaining fractures can be eliminated without significantly affecting the network permeability. This is not dependent on finite-size limitations.

The importance of fractures to fluid flow is not simply related to fracture length or fracture aperture. Figure 5 shows that when fractures are deleted according to flow simulation results, the cumulative length of the conducting backbone of truncated fracture networks decreases almost linearly. This shows, for instance, that it is not exclusively short fractures that are eliminated first. The trend is nearly the same for different values of α. The length l_b here is not the cumulative length of all fractures with some segment in the backbone, but the cumulative length of all the fracture segments in the backbone. Thus, for the original network, the reduction in length by about 20% arises mostly because of eliminating segments, not whole fractures. The plots in Fig. 5 end at the point where some sub-networks in the 100 realizations are disconnected entirely.

To understand why the dominant sub-network is sparser when the aperture distribution is broader, we examine one randomly selected realization for each value of α in detail. The only difference among the specific realizations used for different values of α is the aperture distribution. First, we examine the distribution of the values of Q for each fracture in the original fracture network. As presented in Fig. 6, when $\alpha = 1.001$, the fracture network shows strongly

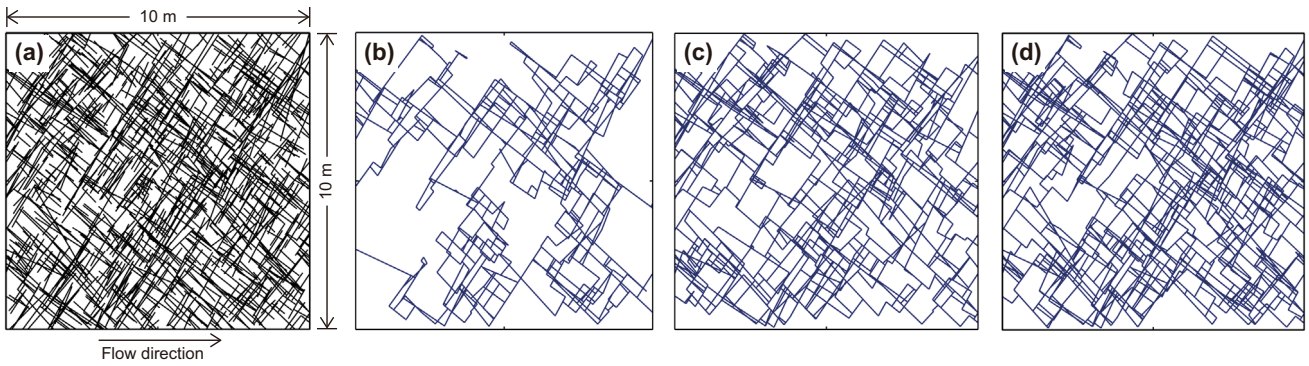

Fig. 4 **a** One realization of the fracture network examined in this study. The size of the fractured region is 10 m × 10 m × 0.01 m. The *left* and *right* boundaries are each at a fixed hydraulic head; the difference in hydraulic head is 1 m. Water flows from *left* to *right*; the *top* and *bottom* edges are no-flow boundaries. **b** Dominant sub-network for one realization with a power-law aperture distribution with $\alpha = 1.001$. **c** Dominant sub-network for one realization with a power-law aperture distribution with $\alpha = 2$. **d** Dominant sub-network for one realization with a power-law aperture distribution with $\alpha = 6$

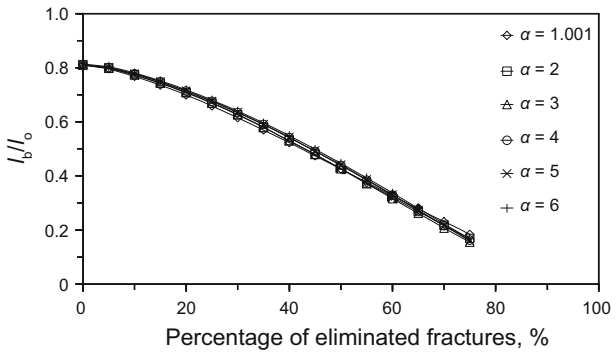

Fig. 5 Length of the backbone of the truncated fracture network (l_b) normalized by the total length of the original fracture network (l_o) plotted against percentage of eliminated fractures, for power-law aperture distributions with exponent $\alpha = 1.001$ to 6. Average trend curve for 100 realizations is shown for each value of α

preferential flow paths: A small portion of the fractures carry much more flow than the others. Specifically, the range in Q for most fractures in the backbone extends over at least five orders of magnitude for $\alpha = 1.001$ (from 4 through 8 in Fig. 6a). For $\alpha = 6$, the value of Q for most fractures lies within a range of about two orders of magnitude (from 5 to 7 in Fig. 6c). Thus, when the aperture distribution is broad, the equivalent permeability is not strongly affected as it is the "unimportant" fractures that are eliminated. As the aperture distribution becomes narrower, flow does not concentrate in a small portion of fractures: Most fractures play a roughly similar role in the flow, which means fewer fractures can be removed without significantly reducing the equivalent network permeability.

The relationship between the aperture and Q for each fracture is shown in Fig. 7. The importance of individual fractures to the overall flow properties of fracture networks cannot be simply related to the aperture of each fracture. There are some fractures with small aperture that carry more flow than fractures with larger aperture. This is true for all the cases with aperture distribution, from narrow to broad.

Similar to the lack of a simple relation between the aperture and Q, there is no clear relationship between the fracture length and the flow each fracture carries (Fig. 8). There are some relatively long fractures that carry very little flow and some short fractures playing a more important role than the longer fractures. Fracture networks with narrow and broad aperture distribution show similar lack of correlation between the fracture length and the flow each fracture carries in Fig. 8.

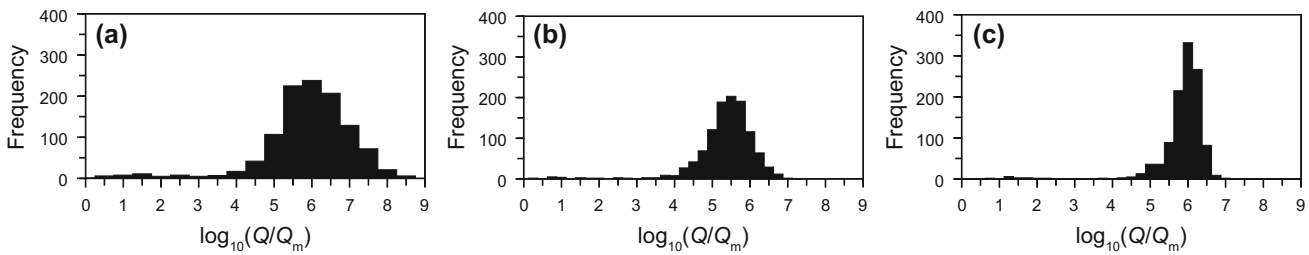

Fig. 6 Histogram of Q for each fracture normalized by the minimum value of Q for all fractures in the backbone (Q_m) in log-10 space: power-law aperture distributions with $\alpha = 1.001$ (**a**), $\alpha = 2$ (**b**), $\alpha = 6$ (**c**). Results of one realization are shown for each value of α

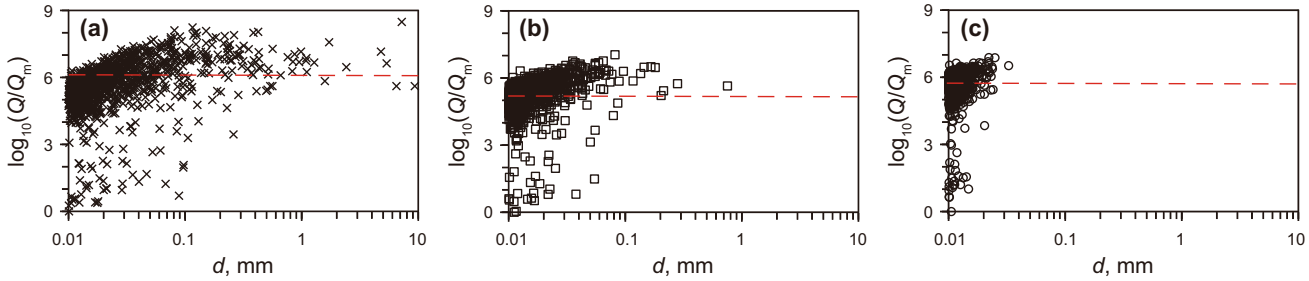

Fig. 7 Q for each fracture normalized by the minimum value of Q for all the fractures in log-10 space plotted against aperture d: power-law aperture distributions with $\alpha = 1.001$ (**a**), $\alpha = 2$ (**b**), $\alpha = 6$ (**c**). Results of one realization are shown for each value of α. The *red dashed line* indicates the value of Q below which the fractures are eliminated while retaining 90% of the original permeability

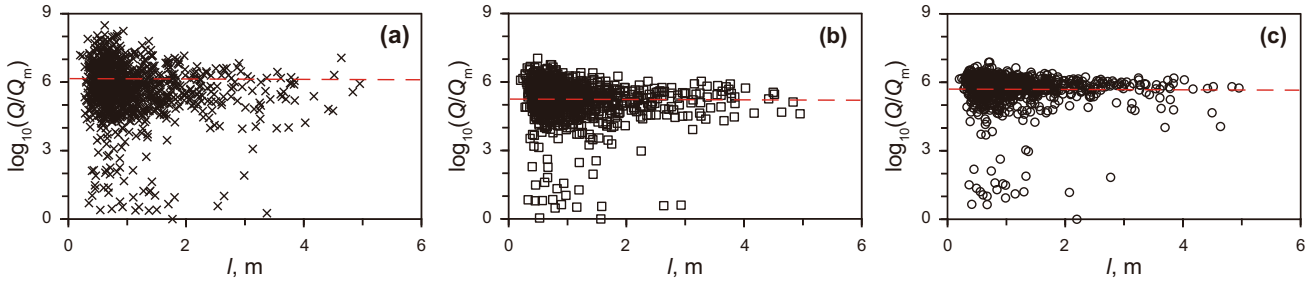

Fig. 8 Q of each fracture normalized by the minimum value of Q in log-10 space plotted against the fracture length l: power-law aperture distributions with $\alpha = 1.001$ (**a**), $\alpha = 2$ (**b**), $\alpha = 6$ (**c**). Results of one realization are shown for each value of α. The *red dashed line* indicates the value of Q below which the fractures are eliminated while retaining 90% of the original permeability

In principle, each individual fracture could play a different role in the original fracture network and the dominant sub-network. Most of the fractures carry nearly the same flow in the original fracture network and the dominant sub-network, however, as shown in Fig. 9. This holds for the aperture distribution ranging from narrow to broad. In the dominant sub-network, some fractures carry more flow and some carry less, compared to the original fracture network. There is no fluid flow through some fractures in the dominant sub-network at all. When some fractures that carry little flow are eliminated from the fracture network, their removal disconnects some other fractures from the backbone. This could happen, for instance, if several fractures carrying little flow feed into one fracture that carries the sum of all their flows. Then the removal of the fractures carrying little flow can lead to the disconnection

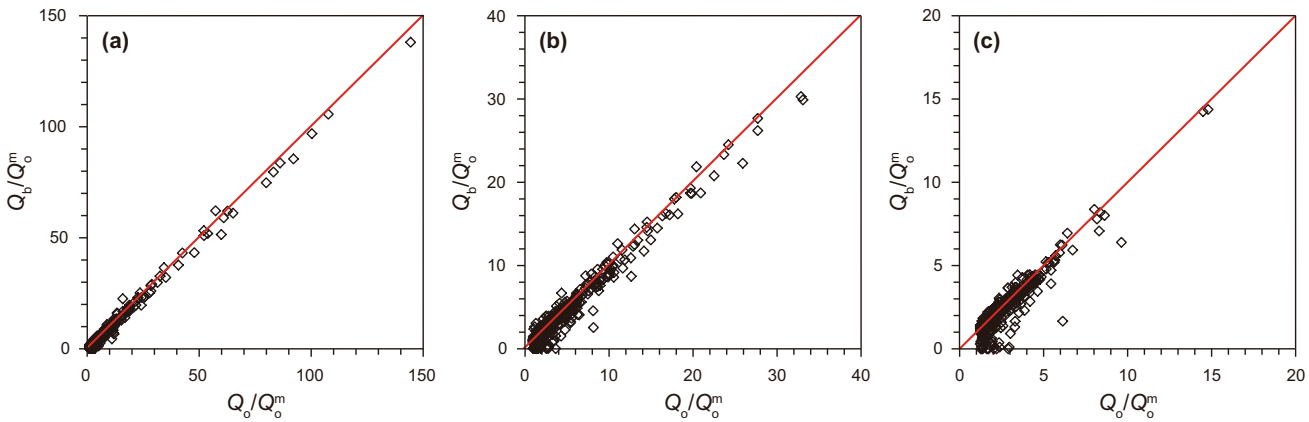

Fig. 9 Comparison of Q for fractures in the original fracture network (Q_o) and in the dominant sub-network (Q_b): power-law aperture distributions with $\alpha = 1.001$ (**a**), $\alpha = 2$ (**b**), $\alpha = 6$ (**c**). Both Q_o and Q_b are normalized by the minimum value of Q in the original fracture network (Q_o^m). Results of one realization are shown for each value of α

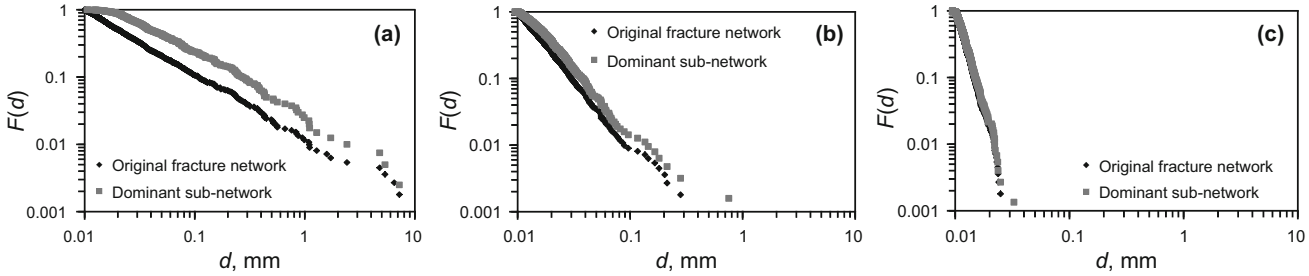

Fig. 10 Comparison of the aperture distribution of the original fracture network and the dominant sub-network: power-law aperture distributions with $\alpha = 1.001$ (**a**), $\alpha = 2$ (**b**), $\alpha = 6$ (**c**). $F(d)$ is the fraction of fractures with aperture (d) larger than the given value. Results of one realization are shown for each value of α

of a fracture that carries more flow from the backbone. However, in fact, there are relatively few fractures disconnected from the backbone in the dominant sub-network.

Figure 10 shows a comparison of the aperture distribution of the dominant sub-network to that of the original fracture network. The plots are similar to each other, which indicate again that the fractures with small aperture are not systematically removed.

We may summarize our arguments of the cases with power-law aperture distributions as follows. For all of the cases with a power-law aperture distribution, at least a portion of fractures can be eliminated without significantly affecting the effective network permeability. The number of fractures that can be removed is strongly affected by the value of α, i.e., the breadth of the aperture distribution. The broader the aperture distribution is, the more fractures can be eliminated without significantly affecting the overall flow behavior. When the aperture distribution is broad enough ($\alpha \leq 2$), the original fracture network behaves as a sparse sub-network, and the total length of the fractures in the sub-network is much shorter than that of the original fracture network. The importance of each fracture to the flow behavior of the entire fracture network cannot be simply related to its aperture or length; some fractures with narrow aperture or short length play a more important role than others with broader aperture or greater length.

3.1.2 Log-normal aperture distribution

Some researchers proposed a log-normal distribution for apertures based on field studies and hydraulic tests (Snow 1970; Long and Billaux 1987; Dverstorp and Andersson 1989; Cacas et al. 1990a, b; Tsang et al. 1996). Fracture network models with log-normal distributions of apertures have been widely used to simulate experiments and derive theoretical relationships (Charlaix et al. 1987; Feng et al. 1987; Long and Billaux 1987; Dverstorp and Andersson 1989; Cacas et al. 1990a, b; Tsang et al. 1996; Margolin et al. 1998; de Dreuzy et al. 2001b). The log-normal

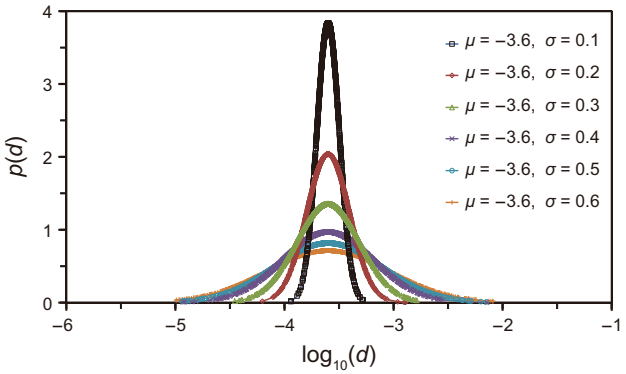

Fig. 11 Probability density function ($p(d)$) for fracture aperture for log-normal distributions with the same mean value but different standard deviations in log-10 space

distribution is specified by the following probability density function:

$$p(d) = \frac{1}{d\log_{10}(\sigma)\sqrt{2\pi}}\exp\left\{-\frac{1}{2}\left(\frac{\log_{10}(d)-\mu}{\sigma}\right)^2\right\} \quad (7)$$

where μ and σ are the mean and the standard deviation in log-10 space. The truncated log-normal distribution has two additional parameters: a minimum and a maximum value of apertures, which are 0.01 and 10 mm, respectively, in this study. Field studies and hydraulic tests found values of σ from 0.1 to 0.3, 0.23, and 0.47 (Snow 1970; Dverstorp and Andersson 1989; Tsang et al. 1996). To test the widest range of feasible values, we test values of σ from 0.1 to 0.6, as illustrated in Fig. 11. As shown in Fig. 11, the upper and lower bounds have little effect on these distributions. The aperture distribution becomes broader as σ increases from 0.1 to 0.6.

In this paper, we mainly show the results for σ with values 0.1, 0.4, and 0.5. The results for σ with additional values examined in this study can be found elsewhere (Gong and Rossen 2015).

Similar to our approach in dealing with the cases of power-law aperture distributions, we first run flow

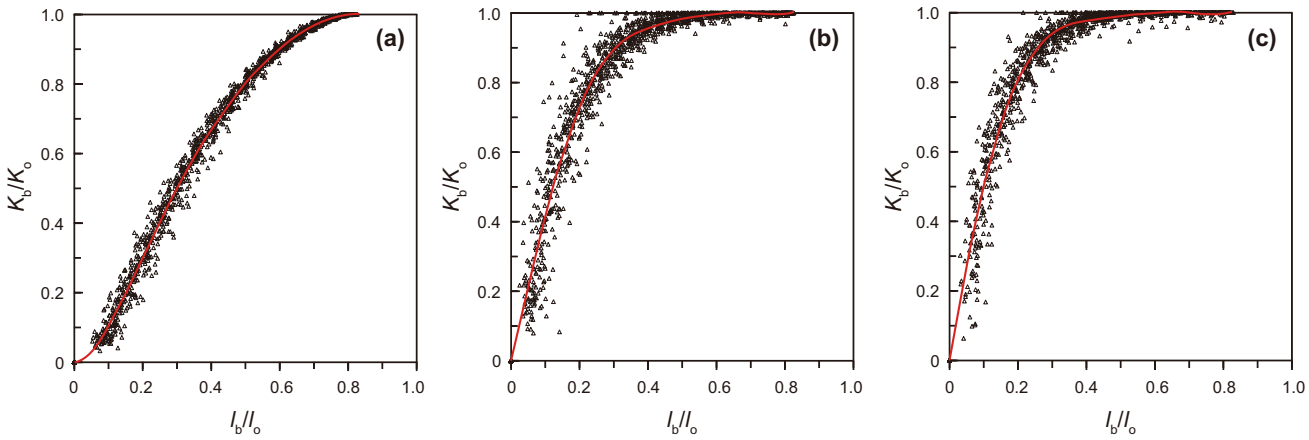

Fig. 12 Sub-network equivalent permeability (K_b) normalized by the equivalent permeability of the original fracture network (K_o), plotted against the length of the backbone of the truncated fracture network (l_b) normalized by the total length of the original fracture network (l_o): log-normal aperture distributions with $\sigma = 0.1$ (**a**), $\sigma = 0.4$ (**b**), $\sigma = 0.5$ (**c**). Results of 100 realizations are shown for each value of σ. The *red curve* is the average trend curve

simulation for each realization and then eliminate fractures based on the flow simulation results, starting with the fracture with the smallest Q. For each sub-network, the equivalent permeability, the cumulative length of the conducting backbone, and the aperture distribution are calculated. The overall trend of the change of the equivalent permeability is obtained over the 100 realizations for each set of parameter values. Figure 12 presents the results for the cases with $\sigma = 0.1$, 0.4, and 0.5, which are typical values observed in field studies. The broader the aperture distribution, the more fractures can be removed from the system while retaining a given fraction of the original network permeability (Fig. 13). For example, to retain 90% of the equivalent permeability of the original network, the cumulative length of the conducting backbone of the dominant sub-network is around 60% of total fracture length of the original fracture network when $\sigma = 0.1$, while the ratio is roughly 35% and 30% when $\sigma = 0.4$ and 0.5, respectively. Clearly, the dominant sub-network which retains 90% of the original equivalent permeability is strongly affected by the aperture distribution. When the standard deviation is larger than 0.4, the aperture distribution is broad enough that most fractures can be eliminated without significantly affecting the equivalent network permeability. The conducting backbone of the dominant sub-network is much sparser than that of the original fracture network (Fig. 14).

As with the cases of power-law aperture distributions, in the cases of log-normal aperture distributions, the length of the backbone of sub-networks decreases nearly linearly with an increasing portion of fractures being eliminated, based on the flow simulation results. As in Fig. 3, the ratio shown in Fig. 15 starts at about 0.8 for zero fractures removed because not all fracture segments in the original

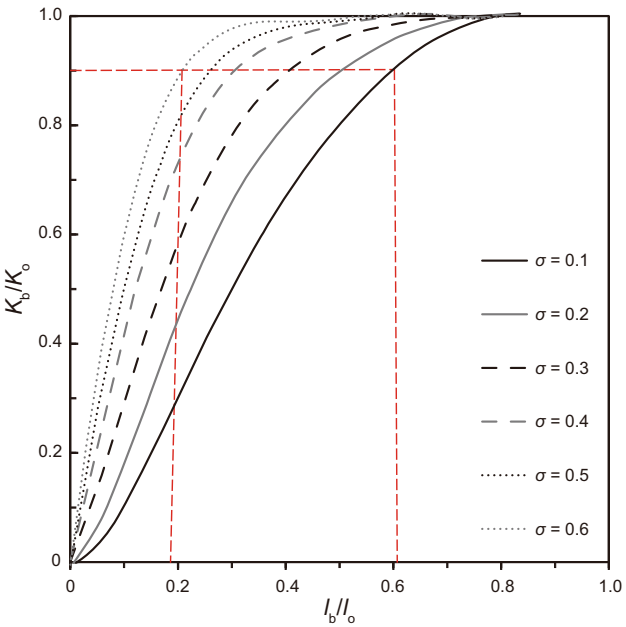

Fig. 13 Average curves from Fig. 12

network are in the backbone. The plots end at the point where some sub-networks are disconnected entirely.

The distributions of Q for fractures in the original networks with log-normal aperture distributions are similar to those with power-law aperture distributions (cf. Fig. 6). When the aperture distribution is narrow ($\sigma = 0.1$), the distribution of Q is also narrow: Most of the fractures carry a similar amount of flow. As a result, when a portion of fractures is eliminated, the equivalent network permeability is strongly affected. As the aperture distribution becomes broader, the distribution of Q is also broader, and there is a small portion of fractures which

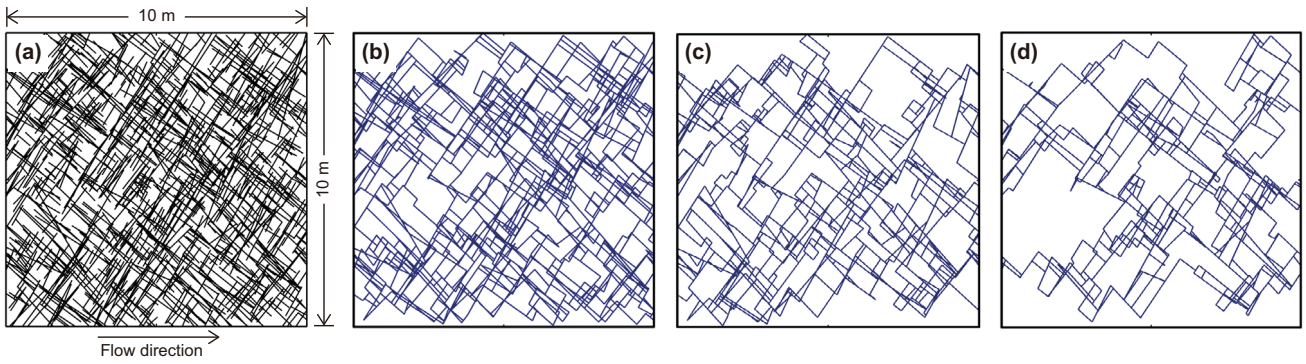

Fig. 14 **a** One realization of the fracture network examined in this study. **b** Dominant sub-network for one realization with a log-normal aperture distribution with $\sigma = 0.1$. **c** Dominant sub-network for one realization with a log-normal aperture distribution with $\sigma = 0.4$. **d** Dominant sub-network for one realization with a log-normal aperture distribution with $\sigma = 0.5$

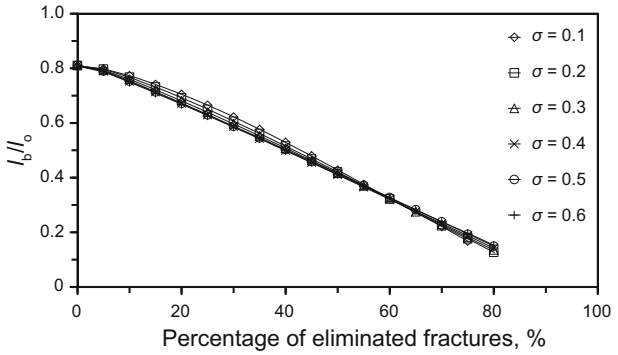

Fig. 15 Length of sub-network backbone (l_b) normalized by the total length of the original fracture network (l_o) plotted against the percentage of eliminated fractures, for the cases of log-normal aperture distributions with the same log-mean value but different log-standard deviations (σ) from 0.1 to 0.6. Average trend curve for 100 realizations is shown for each value of σ

carry much more flow than the others. In other words, the fracture network shows stronger preferential flow paths when the aperture distribution becomes broader. Thus, removing a portion of fractures which carry little flow does not greatly reduce the equivalent network permeability, as the fractures that play a more important role are still in the system.

As presented in Figs. 16 and 17, the flow behavior of each fracture cannot be simply related to either aperture or length. However, compared to the cases with power-law aperture distributions, we find that for most of the fractures, the overall trend is that fractures with larger aperture tend to carry more flow than those with narrower aperture, which is different from the results for the cases with power-law aperture distributions (cf. Fig. 7). We believe a comparison between Figs. 1 and 11 provides the answer: There are many more small fractures (just above the cutoff for fracture aperture) in the power-law distribution than in the log-normal distribution. It may be that it is just as unlikely for a narrow fracture to be important in a power-law distribution, but there are so many of them that some of them do play a role.

Similar to the cases of power-law aperture distributions, most fractures carry similar flow when they are in the dominant sub-network and in the original fracture network, which indicates that they behave similarly.

Figure 18 presents the aperture distribution of the original fracture network and that of the dominant sub-network for one realization for each value of σ. Compared to the original fracture network, the dominant sub-network lacks a portion of small fractures which means that fractures with small aperture are eliminated systematically. The aperture distributions are different from each other.

In summary, for the log-normal aperture distributions, we conclude that when the aperture distribution is broad enough ($\sigma \geq 0.4$), most of the fractures can be taken out without significantly affecting the equivalent network permeability. In contrast to the cases of power-law aperture distributions, the fractures with larger aperture tend to play a more important role for the flow behavior of the fracture network, although the flow carried by each fracture cannot be simply related to the fracture aperture.

3.2 Aperture proportional to fracture length

Field measurements and theoretical studies raise the possibility of a relationship between fracture aperture and fracture length (Stone 1984; Hatton et al. 1994; Vermilye and Scholz 1995; Johnston and McCaffrey 1996; Renshaw and Park 1997). Both nonlinear and linear relationships have been proposed in previous studies based on elastic theory and field data. Here we assume that the aperture of each fracture is uniform and proportional to fracture length:

$$d = Cl \tag{8}$$

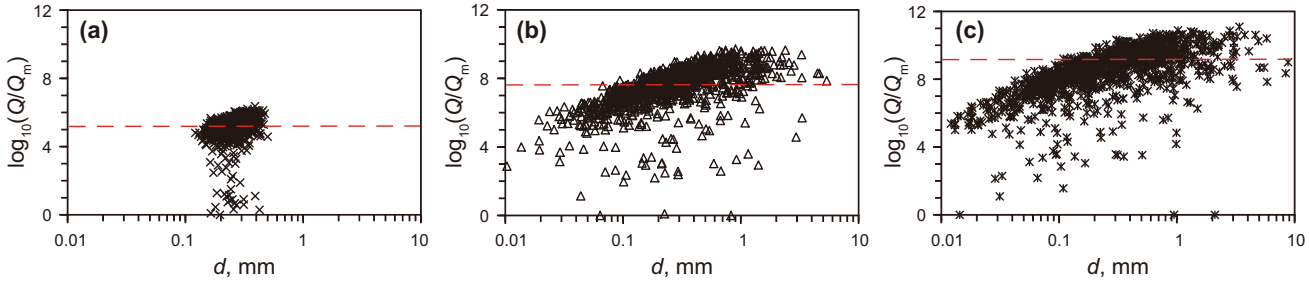

Fig. 16 Q for each fracture normalized by the minimum value of Q for all the fractures in log-10 space plotted against fracture aperture: log-normal aperture distributions with $\sigma = 0.1$ (**a**), $\sigma = 0.4$ (**b**), $\sigma = 0.5$ (**c**). Results of one realization are shown for each value of σ. The *red dashed line* indicates the value of Q below which the fractures are eliminated in this case

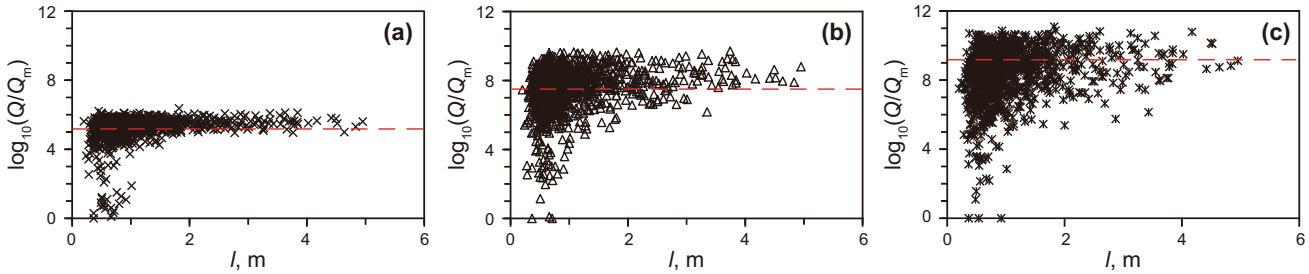

Fig. 17 Q for each fracture normalized by the minimum value of Q for all the fractures in log-10 space plotted against fracture length l: log-normal aperture distributions with $\sigma = 0.1$ (**a**), $\sigma = 0.4$ (**b**), $\sigma = 0.5$ (**c**). Results of one realization are shown for each value of σ. The *red dashed line* indicates the value of Q below which the fractures are eliminated in this case

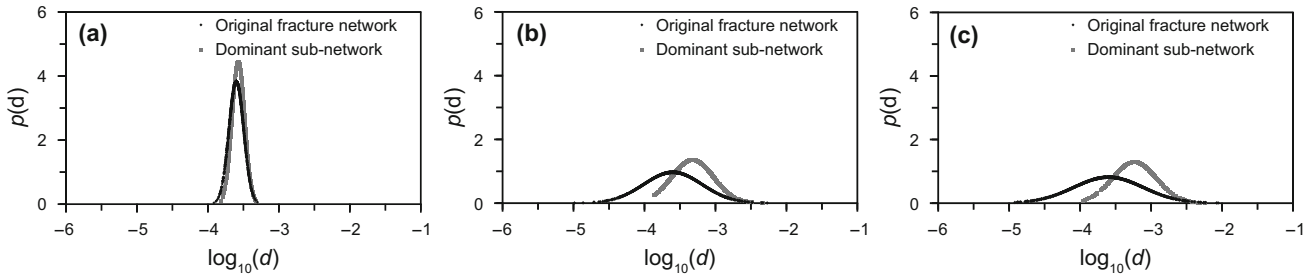

Fig. 18 Comparison of aperture distribution for the original fracture network and the dominant sub-network: log-normal aperture distributions with $\sigma = 0.1$ (**a**), $\sigma = 0.4$ (**b**), $\sigma = 0.5$ (**c**). $p(d)$ is the probability density function. Results of one realization are shown for each value of σ

where d is aperture; C is an empirical coefficient; and l is fracture length. Vermilye and Scholz (1995) suggested the empirical coefficient lies between 1×10^{-3} and 8×10^{-3}. Here for the Mafic^{TM} flow calculations we use 2×10^{-3}. However, since we normalize the properties of the sub-network by those of the original fracture network, the value of C is unimportant to what follows.

As mentioned above, all the cases we test in this study follow a power-law length distribution with exponent $\alpha = 2$, which is truncated between 0.2 and 6 m. Since in this section aperture is proportional to fracture length, the apertures also follow a power-law distribution with exponent $\alpha = 2$ and lie in the range of 0.4 to 12 mm. For the case described above with $\alpha = 2$ and aperture independent of fracture length, the apertures lie mostly in the range of 0.01 to 0.1 mm. Whether or not aperture is dependent on fracture length, the difference between the smallest and the largest values is nearly one order of magnitude, although the absolute values are different. The absolute value does not matter to the normalized results presented below.

Figures 19 and 20 show the sub-network equivalent permeability after elimination of a portion of fractures, where the aperture is, respectively, proportional to and independent of the fracture length. In the two types of cases, the overall flow behavior is roughly similar and the cumulative length of the conducting backbone of the

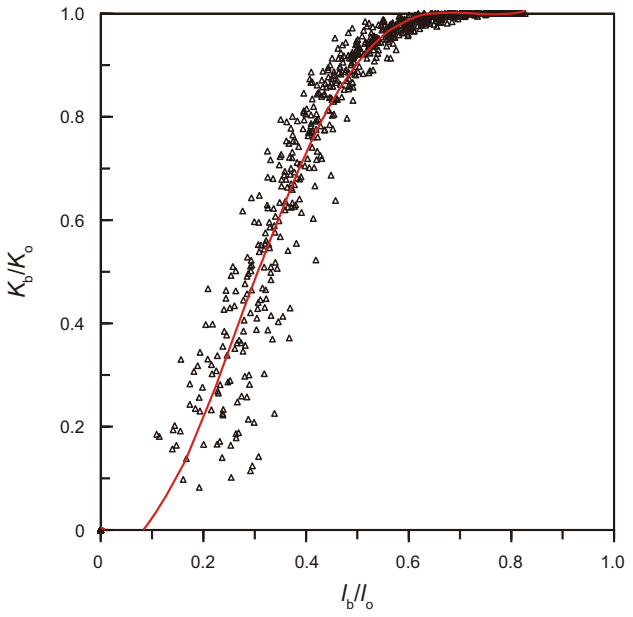

Fig. 19 Sub-network equivalent permeability (K_b) normalized by the equivalent permeability of the original fracture network (K_o), plotted against the length of the backbone of the truncated fracture network (l_b) normalized by the total length of the original fracture network (l_o): aperture is proportional to fracture length. Results of 100 realizations are shown. The *red curve* is the average trend curve

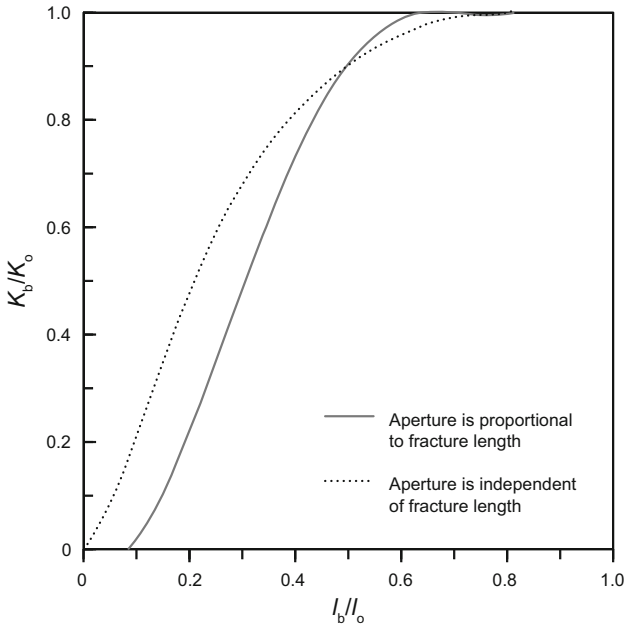

Fig. 20 Average curves from Figs. 2b and 19

dominant sub-networks is approximately 50% of the total fracture length separately.

Figure 21 presents the distribution of Q among fractures for one realization where the aperture is proportional to fracture length. The values of Q distribute more broadly

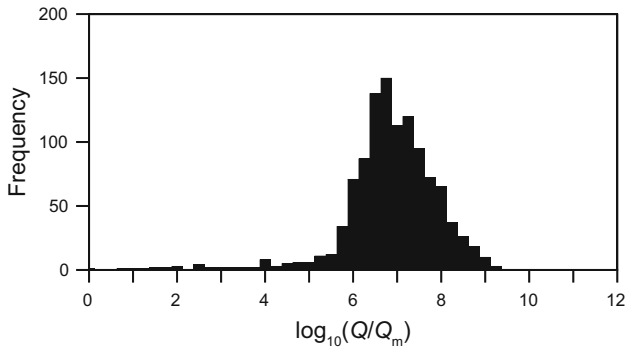

Fig. 21 Histogram of Q of each fracture normalized by the minimum value of Q of all the fractures in log-10 space: aperture is proportional to fracture length. Results of one realization are shown

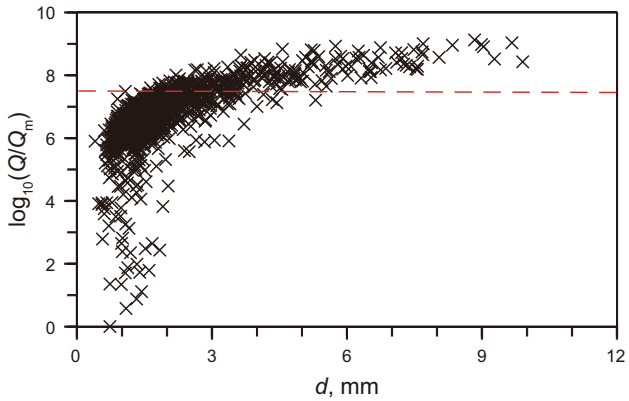

Fig. 22 Q of each fracture normalized by the minimum value of Q of all the fractures in log-10 space plotted against aperture: aperture is proportional to fracture length. Results of one realization are shown. The *red dashed line* indicates the value of Q below which the fractures are eliminated in this case

Table 1 Fracture elimination criteria

Criterion	Description
1	Aperture (d)
2	Length (l)
3	Number of intersections (n)
4	Flow simulation results (q)
5	Aperture × length (dl)
6	Aperture^2 × length (d^2l)
7	Aperture^3 × length (d^3l)
8	Aperture × length^2 (dl^2)
9	Aperture^3/length (d^3/l)
10	Aperture × number of intersections (dn)
11	Length × number of intersections (ln)
12	Aperture × length × number of intersections (dln)

when aperture is proportional to fracture length than when aperture is independent of fracture length (cf. Fig. 6b). In this realization, the original fracture network has 1120

fractures and the sub-network has 633 fractures when the aperture is independent of the length, but only 217 fractures when the aperture is proportional to the fracture length: similar cumulative length, but fewer fractures. This indicates that shorter fractures are eliminated preferentially.

Figure 22 shows the relationships between aperture and Q, which shows that, although there are some fractures with small aperture (shorter fractures) that carry a lot of flow, the overall trend is that fractures with larger aperture (and greater length) tend to carry more flow.

Whether or not aperture is proportional to fracture length, the original fracture network behaves as a sparse network, and the cumulative length of the conducting backbone of the dominant sub-network is roughly half of the total length of the original fracture network. However, in contrast to the cases where the aperture is independent of the fracture length, the fractures with narrower aperture (shorter fractures) tend to be less important to flow in the network than those with larger aperture (longer fractures) when the aperture is proportional to the fracture length.

4 Possibility of identifying the dominant sub-network without doing flow simulation

In this section, we explore possible criteria to obtain a sparse dominant sub-network without doing flow simulations. The results in the previous section show clearly that

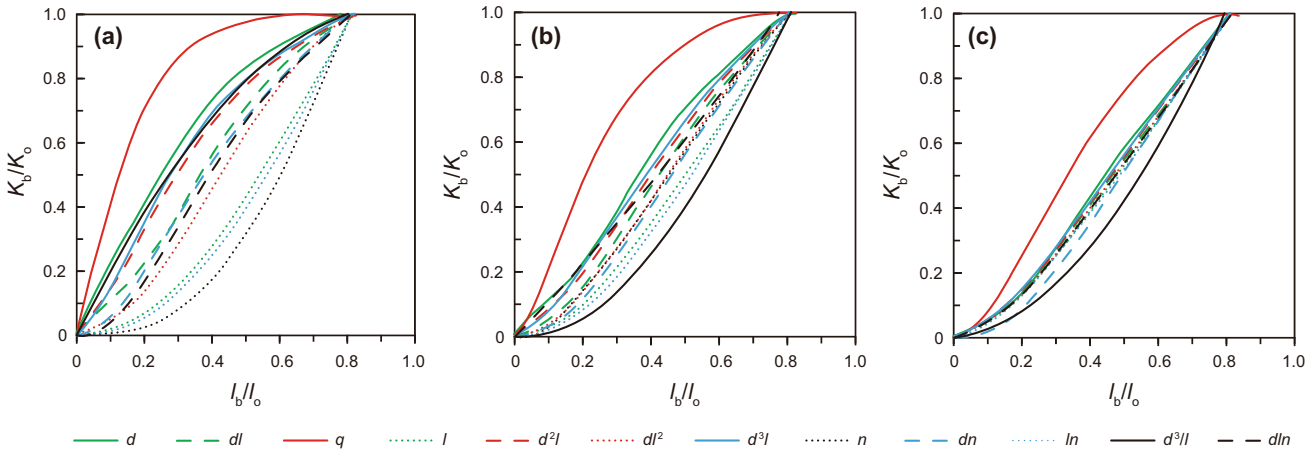

Fig. 23 Sub-network equivalent permeability (K_b) normalized by the equivalent permeability of the original fracture network (K_o), plotted against the length of the backbone of the truncated fracture network (l_b) normalized by the total length of the original fracture network (l_o) for power-law aperture distributions with $\alpha = 1.001$ (**a**), $\alpha = 2$ (**b**), $\alpha = 6$ (**c**). Fractures are eliminated according to different criteria, as indicated

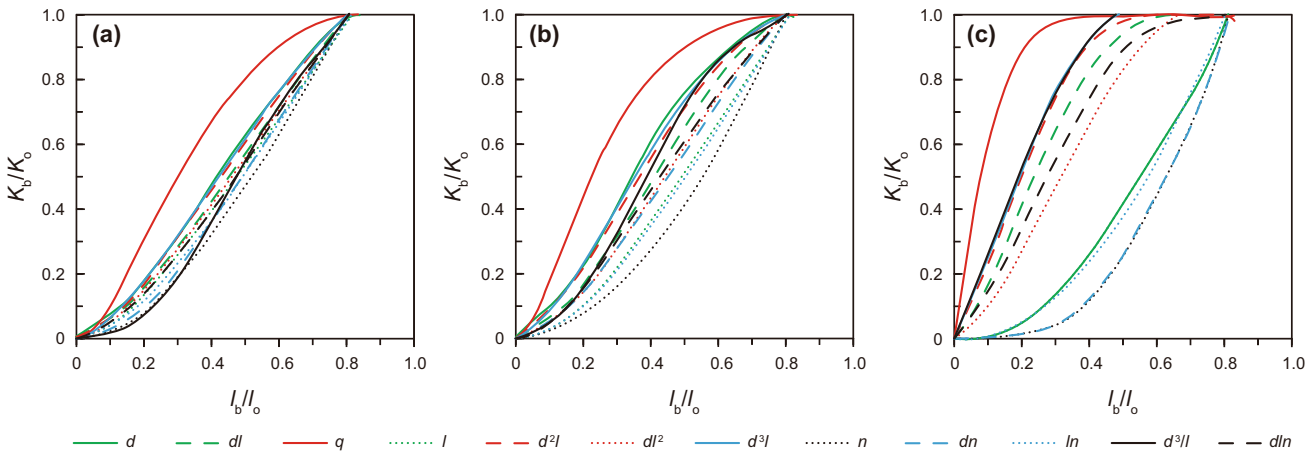

Fig. 24 Sub-network equivalent permeability (K_b) normalized by the equivalent permeability of the original fracture network (K_o), plotted against the length of the backbone of the truncated fracture network (l_b) normalized by the total length of the original fracture network (l_o) for log-normal aperture distributions with $\sigma = 0.1$ (**a**), $\sigma = 0.2$ (**b**), $\sigma = 0.6$ (**c**). Fractures are eliminated according to different criteria, as indicated

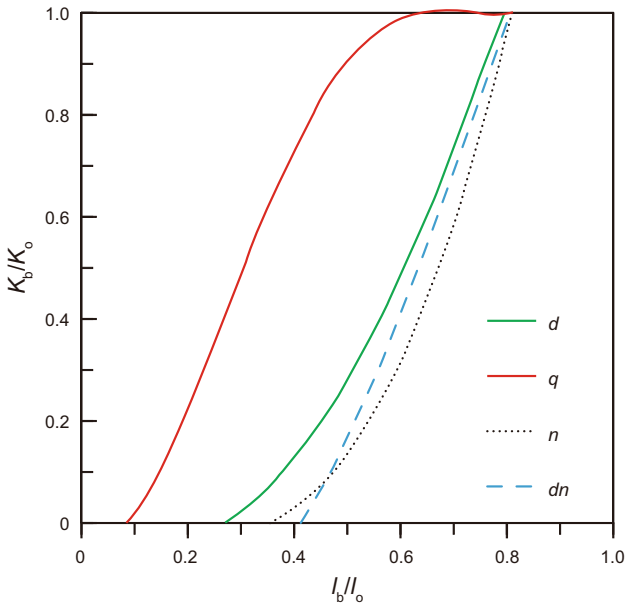

Fig. 25 Sub-network equivalent permeability (K_b) normalized by the equivalent permeability of the original fracture network (K_o), plotted against the length of the backbone of the truncated fracture network (l_b) normalized by the total length of the original fracture network (l_o), for the cases where the aperture is proportional to the fracture length. Fractures are eliminated according to different criteria, as indicated

the aperture distribution has a great influence on the dominant sub-network. Also, fracture length plays an important role in the flow behavior of fracture networks. Besides the aperture and the length, the other factor we consider here is the number of intersections each fracture has with other fractures. It is believed that this term reflects the importance of a fracture to the connectivity of the fracture network (Robinson 1983). We define criteria from these three individual factors and some of their combinations (Table 1). In the previous section, we discussed identifying the dominant sub-network based on flow simulation results. That is, we conduct a flow simulation on the original fracture network and then eliminate the fractures starting with the smallest Q, in order of increasing Q. In this section, we explore the possibility of identifying the dominant sub-network without doing flow simulations first. The fractures are now eliminated according to some fracture property. For example, the fractures are eliminated based on aperture, starting with the smallest aperture, and then in order of increasing aperture.

We compare the effective permeability of the sub-network with a portion of fractures eliminated from the original fracture network using these criteria. Not all the cases examined above are tested here: For the cases with power-law aperture distributions, we examine $\alpha = 1.001$, 2, and 6; for the cases of log-normal aperture distributions, we examine $\sigma = 0.1$, 0.2, and 0.6; we also test the cases where the aperture is proportional to the fracture length.

As presented in Figs. 23 and 24, aperture is a better criterion than the others (more fractures can be eliminated while retaining 90% of the original permeability). For the case in which the aperture is proportional to the fracture length, the results obtained according to the criteria of aperture and fracture length are the same; therefore, only four plots are shown in Fig. 25. Nevertheless, eliminating fractures based on aperture is not nearly as efficient as eliminating fractures based on flow simulations.

5 Conclusions

This work focuses on the effect of fracture aperture distribution on the dominant sub-network that by itself retains 90% of the effective permeability of the original fracture network. A number of aperture distributions are tested: log-normal and power-law distributions (from narrow to broad), and one where the aperture is proportional to the fracture length. If the aperture distribution is broad enough ($\alpha \leq 2$ for power-law aperture distributions and $\sigma \geq 0.4$ for log-normal aperture distributions), most of the fractures can be eliminated without significantly reducing the effective permeability. As the exponent α of a power-law aperture distribution increases or the standard deviation σ of a log-normal aperture distribution decreases, fewer and fewer fractures can be removed without significantly reducing the network equivalent permeability.

The importance of each fracture to the overall flow is not simply related to aperture or length. For the cases of both the log-normal and power-law aperture distributions, and that where the aperture is proportional to the fracture length, there are some fractures with relatively narrow aperture that play a greater role in the overall flow than some others with larger aperture. It is also true that some fractures with relatively large aperture carry much less flow than most of the fractures.

Flow simulations are more effective at identifying the largest sub-network that retains 90% of the original permeability than eliminating fractures based on length, aperture, or number of intersections. Among those properties, eliminating fractures based on aperture is the most efficient choice considered here, but not as efficient as using flow calculations.

References

Aharony A, Stauffer D. Introduction to percolation theory. London: Taylor & Francis; 2003.

Balberg I, Anderson C, Alexander S, et al. Excluded volume and its relation to the onset of percolation. Phys Rev B Condens Matter. 1984;30(7):3933. doi:10.1103/PhysRevB.30.3933.

Balberg I, Berkowitz B, Drachsler G. Application of a percolation model to flow in fractured hard rocks. J Geophys Res Solid Earth. 1991;96(B6):10015–21. doi:10.1029/91JB00681.

Barton CA, Zoback MD. Self-similar distribution and properties of macroscopic fractures at depth in crystalline rock in the Cajon Pass Scientific Drill Hole. J Geophys Res Solid Earth. 1992;97(B4):5181–200. doi:10.1029/91JB01674.

Barton CC, Hsieh PA, Angelier J, et al. Physical and hydrologic-flow properties of fractures: Las Vegas, Nevada–Zion Canyon, Utah–Grand Canyon, Arizona–Yucca Mountain, Nevada July 20–24, 1989. Washington, D.C.: American Geophysical Union; 1989.

Belayneh M, Masihi M, Matthäi S, et al. Prediction of vein connectivity using the percolation approach: model test with field data. J Geophys Eng. 2006;3(3):219. doi:10.1088/1742-2132/3/3/003.

Belfield W, Sovich J. Fracture statistics from horizontal wellbores. In: SPE/CIM/CANMET international conference on recent advances in horizontal well applications; March 20–23: Petroleum Society of Canada; 1994. doi:10.2118/95-06-04.

Berkowitz B. Analysis of fracture network connectivity using percolation theory. Math Geol. 1995;27(4):467–83. doi:10.1007/BF02084422.

Berkowitz B. Characterizing flow and transport in fractured geological media: a review. Adv Water Res. 2002;25(8):861–84. doi:10.1016/S0309-1708(02)00042-8.

Berkowitz B, Balberg I. Percolation theory and its application to groundwater hydrology. Water Resour Res. 1993;29(4):775–94. doi:10.1029/92WR02707.

Berkowitz B, Scher H. Anomalous transport in random fracture networks. Phys Rev Lett. 1997;79(20):4038. doi:10.1103/PhysRevLett.79.4038.

Berkowitz B, Scher H. Theory of anomalous chemical transport in random fracture networks. Phys Rev E Stat Nonlinear Soft Matter Phys. 1998;57(5):5858. doi:10.1103/PhysRevE.57.5858.

Bour O, Davy P. Connectivity of random fault networks following a power law fault length distribution. Water Resour Res. 1997;33(7):1567–83. doi:10.1029/96WR00433.

Cacas M, Ledoux E, Marsily Gd, et al. Modeling fracture flow with a stochastic discrete fracture network: calibration and validation: 1. The flow model. Water Resour Res. 1990a;26(3):479–89. doi:10.1029/WR026i003p00479.

Cacas M, Ledoux E, de Marsily G, et al. Modeling fracture flow with a stochastic discrete fracture network: calibration and validation 2. The Transport Model. Water Resour Res. 1990b;26:491–500. doi:10.1029/WR026i003p00491.

Charlaix E, Guyon E, Roux S. Permeability of a random array of fractures of widely varying apertures. Transp Porous Media. 1987;2(1):31–43. doi:10.1007/BF00208535.

de Dreuzy J-R, Davy P, Bour O. Hydraulic properties of two-dimensional random fracture networks following a power law length distribution: 1. Effective connectivity. Water Resour Res. 2001a;37(8):2065–78. doi:10.1029/2001WR900011.

de Dreuzy J-R, Davy P, Bour O. Hydraulic properties of two-dimensional random fracture networks following a power law length distribution: 2. Permeability of networks based on lognormal distribution of apertures. Water Resour Res. 2001b;37:2079–95. doi:10.1029/2001WR900010.

de Dreuzy J-R, Davy P, Bour O. Hydraulic properties of two-dimensional random fracture networks following power law distributions of length and aperture. Water Resour Res. 2002;38(12):121–9. doi:10.1029/2001WR001009.

Dershowitz B, LaPointe P, Eiben T, et al. Integration of discrete feature network methods with conventional simulator approaches. SPE Reserv Eval Eng. 2000;3(2):165–70. doi:10.2118/62498-PA.

Dershowitz B, LaPointe P, Eiben T, et al. User documentation for FracMan. Seattle: Golder Associates Inc.; 2011.

Dverstorp B, Andersson J. Application of the discrete fracture network concept with field data: possibilities of model calibration and validation. Water Resour Res. 1989;25(3):540–50. doi:10.1029/WR025i003p00540.

Feng S, Halperin B, Sen P. Transport properties of continuum systems near the percolation threshold. Phys Rev B: Condens Matter. 1987;35(1):197. doi:10.1103/PhysRevB.35.197.

Gong J, Rossen WR. Modeling flow in naturally fractured reservoirs: effect of fracture aperture distribution on dominant sub-network for flow. TU Delft: Dataset; 2015.

Hatton C, Main I, Meredith P. Non-universal scaling of fracture length and opening displacement. Nature. 1994;367(6459):160–2. doi:10.1038/367160a0.

Hestir K, Long J. Analytical expressions for the permeability of random two-dimensional Poisson fracture networks based on regular lattice percolation and equivalent media theories. J Geophys Res Solid Earth. 1990;95(B13):21565–81. doi:10.1029/JB095iB13p21565.

Johnston J, McCaffrey K. Fractal geometries of vein systems and the variation of scaling relationships with mechanism. J Struct Geol. 1996;18(2):349–58. doi:10.1016/S0191-8141(96)80055-1.

Katz A, Thompson A. Prediction of rock electrical conductivity from mercury injection measurements. J Geophys Res Solid Earth. 1987;92(B1):599–607. doi:10.1029/JB092iB01p00599.

Lee SH, Lough MF, Jensen CL. Hierarchical modeling of flow in naturally fractured formations with multiple length scales. Water Resour Res. 2001;37(3):443–55. doi:10.1029/2000WR900340.

Long J, Billaux DM. From field data to fracture network modeling: an example incorporating spatial structure. Water Resour Res. 1987;23(7):1201–16. doi:10.1029/WR023i007p01201.

Margolin G, Berkowitz B, Scher H. Structure, flow, and generalized conductivity scaling in fracture networks. Water Resour Res. 1998;34(9):2103–21. doi:10.1029/98WR01648.

Marrett R. Aggregate properties of fracture populations. J Struct Geol. 1996;18(2):169–78. doi:10.1016/S0191-8141(96)80042-3.

Masihi M, King PR, Nurafza PR. Fast estimation of performance parameters in fractured reservoirs using percolation theory. In: SPE Europec/EAGE annual conference, 13–16 June, Madrid, Spain; 2005. doi:10.2118/94186-MS.

Masihi M, King PR, Nurafza PR. Connectivity prediction in fractured reservoirs with variable fracture size: analysis and validation. SPE J. 2008;13(01):88–98. doi:10.2118/100229-MS.

Matthai SK, Belayneh M. Fluid flow partitioning between fractures and a permeable rock matrix. Geophys Res Lett. 2004;31(7):L07602. doi:10.1029/2003GL019027.

Matthai SK, Nick HM. Upscaling two-phase flow in naturally fractured reservoirs. AAPG Bull. 2009;93(11):1621–32.

Neretnieks I. Solute transport in fractured rock: applications to radionuclide waste repositories. Flow and contaminant transport in fractured rock. London: Academic Press Limited; 1993. p. 39–127.

Neretnieks I, Eriksen T, Tähtinen P. Tracer movement in a single fissure in granitic rock: some experimental results and their interpretation. Water Resour Res. 1982;18(4):849–58. doi:10.1029/WR018i004p00849.

Nick HM, Paluszny A, Blunt MJ, et al. Role of geomechanically grown fractures on dispersive transport in heterogeneous geological formations. Phys Rev E. 2011;84(5):056301.

Nicol A, Walsh J, Watterson J, et al. Fault size distributions—Are they really power-law? J Struct Geol. 1996;18(2):191–7. doi:10.1016/S0191-8141(96)80044-7.

Nordqvist AW, Tsang YW, Tsang C-F, et al. Effects of high variance of fracture transmissivity on transport and sorption at different scales in a discrete model for fractured rocks. J Contam Hydrol. 1996;22(1):39–66. doi:10.1016/0169-7722(95)00064-X.

Odling NE. Scaling and connectivity of joint systems in sandstones from western Norway. J Struct Geol. 1997;19(10):1257–71. doi:10.1016/S0191-8141(97)00041-2.

Renshaw CE, Park JC. Effect of mechanical interactions on the scaling of fracture length and aperture. Nature. 1997;386(6624):482–4. doi:10.1038/386482a0.

Robinson P. Connectivity of fracture systems-a percolation theory approach. J Phys A: Math Gen. 1983;16(3):605. doi:10.1088/0305-4470/16/3/020.

Robinson P. Numerical calculations of critical densities for lines and planes. J Phys A: Math Gen. 1984;17(14):2823. doi:10.1088/0305-4470/17/14/025.

Rouleau A, Gale J. Statistical characterization of the fracture system in the Stripa granite, Sweden. Int J Rock Mech Min Sci. 1985;22(6):353–67. doi:10.1016/0148-9062(85)90001-4.

Sahimi M. Flow and transport in porous media and fractured rock: from classical methods to modern approaches. New York: Wiley; 2011.

Saidi AM. Reservoir engineering of fractured reservoirs (fundamental and practical aspects). Paris: Total Edition Press; 1987.

Salimi H. Physical aspects in upscaling of fractured reservoirs and improved oil recovery prediction. TU Delft: Delft University of Technology; 2010.

Segall P, Pollard DD. Joint formation in granitic rock of the Sierra Nevada. Geol Soc Am Bull. 1983;94(5):563–75. doi:10.1130/0016-7606(1983)94<563:JFIGRO>2.0.CO;2.

Snow DT. The frequency and apertures of fractures in rock. Int J Rock Mech Min Sci. 1970;7(1):23–40. doi:10.1016/0148-9062(70)90025-2.

Stone D. Sub-surface fracture maps predicted from borehole data: an example from the Eye-Dashwa pluton, Atikokan, Canada. Int J Rock Mech Min Sci. 1984;21(4):183–94. doi:10.1016/0148-9062(84)90795-2.

Tsang C, Neretnieks I. Flow channeling in heterogeneous fractured rocks. Rev Geophys. 1998;36(2):275–98. doi:10.1029/97RG03319.

Tsang Y, Tsang C. Channel model of flow through fractured media. Water Resour Res. 1987;23(3):467–79. doi:10.1029/WR023i003p00467.

Tsang Y, Tsang C, Hale F, et al. Tracer transport in a stochastic continuum model of fractured media. Water Resour Res. 1996;32(10):3077–92. doi:10.1029/96WR01397.

Tsang Y, Tsang C, Neretnieks I, et al. Flow and tracer transport in fractured media: a variable aperture channel model and its properties. Water Resour Res. 1988;24(12):2049–60. doi:10.1029/WR024i012p02049.

van Golf-Racht TD. Fundamentals of fractured reservoir engineering. Amsterdam: Elsevier; 1982.

Vermilye JM, Scholz CH. Relation between vein length and aperture. J Struct Geol. 1995;17(3):423–34. doi:10.1016/0191-8141(94)00058-8.

Wong TF, Fredrich JT, Gwanmesia GD. Crack aperture statistics and pore space fractal geometry of Westerly granite and Rutland quartzite: implications for an elastic contact model of rock compressibility. J Geophys Res Solid Earth. 1989;94(B8):10267–78. doi:10.1029/JB094iB08p10267.